

Imaging endoplasmic reticulum calcium with a fluorescent biosensor in transgenic mice

Manami Hara, Vytautas Bindokas, James P. Lopez, Kelly Kaihara, Luis R. Landa, Jr., Mark Harbeck and Michael W. Roe

Am J Physiol Cell Physiol 287:932-938, 2004. First published May 26, 2004;
doi:10.1152/ajpcell.00151.2004

You might find this additional information useful...

This article cites 21 articles, 9 of which you can access free at:

<http://ajpcell.physiology.org/cgi/content/full/287/4/C932#BIBL>

This article has been cited by 1 other HighWire hosted article:

A cAMP and Ca²⁺ coincidence detector in support of Ca²⁺-induced Ca²⁺ release in mouse pancreatic {beta} cells

G. Kang, O. G. Chepurny, M. J. Rindler, L. Collis, Z. Chepurny, W.-h. Li, M. Harbeck, M. W. Roe and G. G. Holz

J. Physiol., July 1, 2005; 566 (1): 173-188.

[\[Abstract\]](#) [\[Full Text\]](#) [\[PDF\]](#)

Updated information and services including high-resolution figures, can be found at:

<http://ajpcell.physiology.org/cgi/content/full/287/4/C932>

Additional material and information about *AJP - Cell Physiology* can be found at:

<http://www.the-aps.org/publications/ajpcell>

This information is current as of May 28, 2010 .

Imaging endoplasmic reticulum calcium with a fluorescent biosensor in transgenic mice

Manami Hara,¹ Vytautas Bindokas,² James P. Lopez,¹ Kelly Kaihara,¹
Luis R. Landa, Jr.,¹ Mark Harbeck,¹ and Michael W. Roe¹

¹Department of Medicine and ²Department of Neurobiology, Pharmacology,
and Physiology, The University of Chicago, Chicago, Illinois 60637

Submitted 19 March 2004; accepted in final form 21 May 2004

Hara, Manami, Vytautas Bindokas, James P. Lopez, Kelly Kaihara, Luis R. Landa, Jr., Mark Harbeck, and Michael W. Roe. Imaging endoplasmic reticulum calcium with a fluorescent biosensor in transgenic mice. *Am J Physiol Cell Physiol* 287: C932–C938, 2004. First published May 26, 2004; 10.1152/ajpcell.00151.2004.—The use of biosynthetic fluorescent sensors is an important new approach for imaging Ca²⁺ in cells. Genetically encoded indicators based on green fluorescent protein, calmodulin, and fluorescence resonance energy transfer (FRET) have been utilized to measure Ca²⁺ in nonmammalian transgenic organisms and provide information about the organization and regulation of Ca²⁺ signaling events in vivo. However, expression of biosynthetic FRET-based Ca²⁺ indicators in transgenic mammals has proven to be problematic. Here, we report transgenic expression of an endoplasmic reticulum (ER) Ca²⁺ biosensor in mouse pancreas. We targeted expression of a yellow cameleon3.3er (YC3.3er) transgene with mouse insulin I promoter. YC3.3er protein expression was limited to pancreatic β -cells within islets of Langerhans and absent in the exocrine pancreas and other tissues. Animals developed and matured normally; sensor expression was unaffected by age. Glucose tolerance in transgenic mice was also unaffected, indicating the transgenic biosensor did not impair endocrine pancreas function. ER Ca²⁺ responses after administration of thapsigargin, carbachol, and glucose were measured in individual β -cells of intact islets using confocal microscopy and confirmed the function of the biosensor. We conclude that controlling transgene transcription with a cell-specific promoter permits transgenic expression of FRET-based Ca²⁺ sensors in mammals and that this approach will facilitate real-time optical imaging of signal transduction events in living tissues.

intracellular calcium; cameleon; fluorescence resonance energy transfer

QUANTITATIVE IMAGING OF SPATIAL and temporal gradients of intracellular Ca²⁺ concentration is essential to furthering our knowledge of Ca²⁺-mediated signal transduction and the wide range of Ca²⁺-dependent cellular functions (2, 3, 17). The advent of genetically targeted biosynthetic sensor technology has significantly increased our ability to study complex signaling events in cells with unprecedented temporal and spatial resolution. Many genetically encoded Ca²⁺ indicators based on Ca²⁺-dependent changes in fluorescence resonance energy transfer (FRET) or sensor conformation are now available that provide quantitative visualization of ion fluxes in specific subcompartments of cells (1, 6, 13, 17). Although this technology has the potential for advancing our understanding of signaling in mammals in vivo, applications of fluorescent Ca²⁺

biosensors have been confined to evaluation of mammalian cells and cell lines in vitro.

Expression of these probes in intact mammalian tissues has proven difficult. One of the major impediments has been the lack of an effective method to deliver biosensor cDNA to cells within a living mammal; this cannot be accomplished effectively and reproducibly with liposomal, electroporation, viral, or ballistic methods but conceivably could be attained using a transgenic approach. Biosynthetic fluorescent cameleon and camgaroo Ca²⁺ sensors based on green fluorescent protein (GFP) and the Ca²⁺ binding protein, calmodulin (13, 17), have been engineered to label specific populations of cells within intact tissues in nonmammalian transgenic organisms (*Caenorhabditis elegans*, *Drosophila melanogaster*, and *Danio rerio*) (5, 9–11, 16, 20, 21). No mammalian transgenic expression of a FRET-based Ca²⁺ biosensor, however, has been reported. In this paper we demonstrate transgenic expression of yellow cameleon3.3er (YC3.3er), a biosynthetic indicator of endoplasmic reticulum Ca²⁺ (6), in endocrine cells of mouse pancreas. Our studies demonstrate the feasibility of applying FRET biosensor imaging technology to transgenic mammalian cell systems and suggest that this approach may be used for real-time visualization of cell signaling in living tissues.

MATERIALS AND METHODS

Transgene construction. The mouse insulin I gene promoter (MIP)-YC3.3-er transgenic construct was assembled using an 8.3-kb fragment of MIP, the 2-kb coding region of YC3.3er, and a 2-kb fragment of the human growth hormone (hGH) cassette gene for high-level expression (6, 7, 14, 15). The 12.3-kb MIP-YC3.3-er-hGH fragment was isolated from the vector by digestion of the plasmid construct with *Hind*III and *Sfi*I and agarose gel electrophoresis. The fragment was further purified using an Elutip-D column (Schleicher & Schuell, Keene, NH).

MIP-YC3.3-er transgenic mice. The purified transgene DNA was microinjected into the pronuclei of CD-1 mice at the Transgenic Mouse/ES Core Facility of the University of Chicago Diabetes Research and Training Center. The transgene was maintained on the CD-1 background, and mice were housed under specific pathogen-free (SPF) conditions with free access to food and water. Tail DNA from potential founder mice was screened for the presence of the transgene by PCR using forward and reverse primers 5'-GACAACCTACTACCTGAGC-TAC-3' and 5'-ACTGGGCTTACATGGCGATACTC-3', respectively. Whole pancreata of F1 progeny were visualized with an Olympus SZX12 stereomicroscope (Olympus, Melville, NY) in bright-field and fluorescence illumination modes. All the procedures involving mice were approved by the University of Chicago Institutional Animal Care and Use Committee.

Address for reprint requests and other correspondence: M. W. Roe, Dept. of Medicine MC1027, The Univ. of Chicago, 5841 South Maryland Ave., Chicago, IL 60637 (E-mail: mroe@medicine.bsd.uchicago.edu).

The costs of publication of this article were defrayed in part by the payment of page charges. The article must therefore be hereby marked "advertisement" in accordance with 18 U.S.C. Section 1734 solely to indicate this fact.

Glucose tolerance testing. Intraperitoneal glucose tolerance tests were performed after a 4-h fast. Blood was sampled from the tail vein before and 30, 60, 90, and 120 min after intraperitoneal injection of 2 mg/g body wt of dextrose. Glucose levels were measured using a Precision Q.I.D. Glucometer (MediSense, Waltham, MA).

Isolation of islets of Langerhans. Pancreatic islets were isolated as described (7). Briefly, the pancreas was inflated with a solution containing 0.3 mg/ml collagenase (Type XI; Sigma, St. Louis, MO) in Hanks' balanced salt solution, injected via the pancreatic duct. The inflated pancreas was removed, incubated at 37°C for 10 min, and shaken vigorously to disrupt the tissue. After differential centrifugation through a Ficoll gradient to separate islets from acinar tissue, the islets were washed and placed on 25-mm glass coverslips. Islets were cultured in RPMI 1640 supplemented with 10% (vol/vol) fetal bovine serum, 100 U/ml penicillin, and 100 µg/ml streptomycin and incubated in a humidified incubator at 37°C in 95% air and 5% CO₂. All imaging studies were performed 2–5 days after isolation.

Immunofluorescence microscopy. Sections (6 µm in thickness) from paraffin-embedded pancreatic tissue were incubated with monoclonal anti-GFP antibody (Sigma) to detect the expression of MIP-YC3.3-er, polyclonal anti-porcine insulin antibody to identify β-cells, and a combination of polyclonal anti-glucagon, anti-somatostatin, and anti-pancreatic polypeptide (PP) antibodies to identify α-, δ-, and PP cells, respectively (DakoCytomation, Carpinteria, CA). The endoplasmic reticulum (ER) was labeled with a polyclonal anti-glucose-regulated protein 94 (GRP94) antibody (Stressgen, Victoria, BC, Canada). Biotin-streptavidin-conjugated anti-mouse IgG and Cy2-conjugated streptavidin anti-mouse and Texas Red-conjugated anti-guinea pig/rabbit IgG secondary antibodies were used for MIP-YC3.3-er and insulin, respectively. Cy5-conjugated secondary antibody was used for non-β-cells and GRP94 (Jackson ImmunoResearch Laboratory, West Grove, PA). The stained sections were visualized with a Leica SP2 AOBS confocal microscope.

Confocal microscopy of isolated islets. Laser scanning confocal images were collected on a Leica SP2 AOBS spectral confocal microscope system using a ×63 NA1.3 glycerol objective, viewing coverslip preparations held at 37°C on the DMIRE2 inverted scope. Excitation illumination was generated by a 405-nm laser, and simultaneous emission was detected at 453–505 nm and 525–600 nm for enhanced cyan fluorescent protein (ECFP; FRET donor) and citrine (FRET acceptor), respectively. Image stacks were reconstructed with Image J software (National Institutes of Health, Bethesda, MD).

ER Ca^{2+} measurements. We measured biosensor function using real-time spinning disk optical confocal microscopy. Islets were placed into a microperfusion chamber mounted on an inverted epifluorescence microscope (TE-2000U, Nikon) equipped with a CARV spinning disk confocal system (Atto). Individual islets were visualized with a ×20 or ×40 fluorescent objective. Biosensor fluorescence excitation light was 440 nm and attenuated 50–90% using neutral density filters. Emitted fluorescence at 535 nm (citrine, FRET acceptor) and 485 nm (ECFP, FRET donor) was measured using a computer-controlled high-speed filter wheel (Lambda 10-2 Optical Filter Changer, Sutter Instruments, Novato, CA); the time for changing emission filters was 60 ms. Images (100- to 250-ms exposure) were captured with a 16-bit Cascade 650 digital camera (Roper Instruments) at 10-s intervals. Imaging data acquisition and analysis were accomplished using MetaMorph/MetaFluor software (Universal Imaging). Data were expressed as background subtracted intensities of the FRET acceptor and donor fluorophores and ratio of the FRET acceptor to FRET donor emission (Ratio 535/485). In addition, data were normalized to the average baseline value of Ratio 535/485 (Relative Ratio) to facilitate comparisons between responses of different cells. In all experiments, islets were superfused with warmed (37°C) buffered salt solutions consisting of (in mM) 119 NaCl, 4.7 KCl, 2.5 CaCl₂, 1 MgCl₂, 1 KH₂PO₄, 25 NaHCO₃ or 10 HEPES-NaOH (pH 7.40), and 2–20 glucose.

Statistical analysis. Comparisons between groups were analyzed by ANOVA (StatView Software, SAS Institute, Cary, NC), and differences were considered to be significant at $P < 0.05$.

RESULTS

We generated transgenic mice expressing YC3.3-er specifically in pancreatic β-cells with a transgene construct similar to one used for transgenic expression of GFP (7). Specific cell targeting of the transgene was determined by the MIP; inclusion of a 2-kb fragment of the hGH cassette gene produced high-level expression (7, 14, 15). The MIP/hGH construct has been shown to generate transgenic mice with GFP expressed exclusively in pancreatic β-cells and not in brain, fat, skeletal or smooth muscle, gastrointestinal cells, kidney, liver, heart, spleen, or cells of the reproductive system (7). The 12.3-kb MIP-YC3.3er transgene DNA (Fig. 1A) was microinjected into pronuclei of CD-1 mice. We obtained four male founders (MIP-YC3.3-er-5, -21, -27, and -40) that were genotypically positive for the transgene. After crossing the founders with wild-type CD-1 mice, only the F1 progeny from the MIP-YC3.3-er-21 founder demonstrated detectable fluorescence.

Using stereomicroscopy, we found protein expression of MIP-YC3.3-er in the pancreata of F1 neonates (as early as 1 day after birth) and adult mice. At the time of writing this report, our colony contains MIP-YC3.3-er-positive mice 17 wk of age, indicating that transgene expression is retained as the animals age. Stereoscopic bright-field and fluorescence imaging (Fig. 1, B and C) and laser scanning confocal microscopy (data not shown) demonstrated that expression of the fluorescent biosensor was restricted to islets of Langerhans. We did not observe MIP-YC3.3-er fluorescence in stomach, spleen, liver, or duodenum. The islet-specific pattern of MIP-YC3.3-er expression was indistinguishable from our previous transgenic mouse line, Tg(MIP-GFP)6729Hara, generated by using a similar MIP/hGH construct to drive expression of GFP specifically in insulin-secreting β-cells (7).

The MIP-YC3.3-er mice developed normally. Body weight and blood glucose levels of 6- and 8-wk-old transgenic animals were not significantly different from age-matched CD-1 control mice ($P > 0.05$; $n = 6$ mice from each group). The average ± SE body weight of 6-wk-old mice was 19.6 ± 2.0 g and 20.5 ± 1.8 g in the transgenic and wild-type mice, respectively. The average ± SE fasting blood glucose concentration in transgenic and wild-type mice was 158.0 ± 9.1 mg/dl and 173.0 ± 4.9 mg/dl, respectively. At 8 wk, the average ± SE fasting blood glucose in the transgenic mice was 166.6 ± 11.2 mg/dl. Intraperitoneal glucose tolerance tests performed in 6-wk-old (Fig. 1D) and 8-wk-old (data not shown) mice also demonstrated no significant differences ($P > 0.05$).

We used laser scanning confocal microscopy to illustrate the expression of the biosensor in paraffin-embedded pancreas sections (Fig. 2) and in single intact live islets of Langerhans (Fig. 3) from MIP-YC3.3-er mice. Immunofluorescence confocal microscopy revealed overlap between the ER Ca^{2+} indicator and insulin immunoreactivity (Fig. 2, A–C). There was no evidence of MIP-YC3.3-er expression in islet α-, δ-, and PP cells (Fig. 2, D–F). These results suggest that MIP-YC3.3-er is expressed only in the insulin-secreting β-cells. Double immunostaining showed that the subcellular distribution of MIP-YC3.3-er in β-cells (Fig.

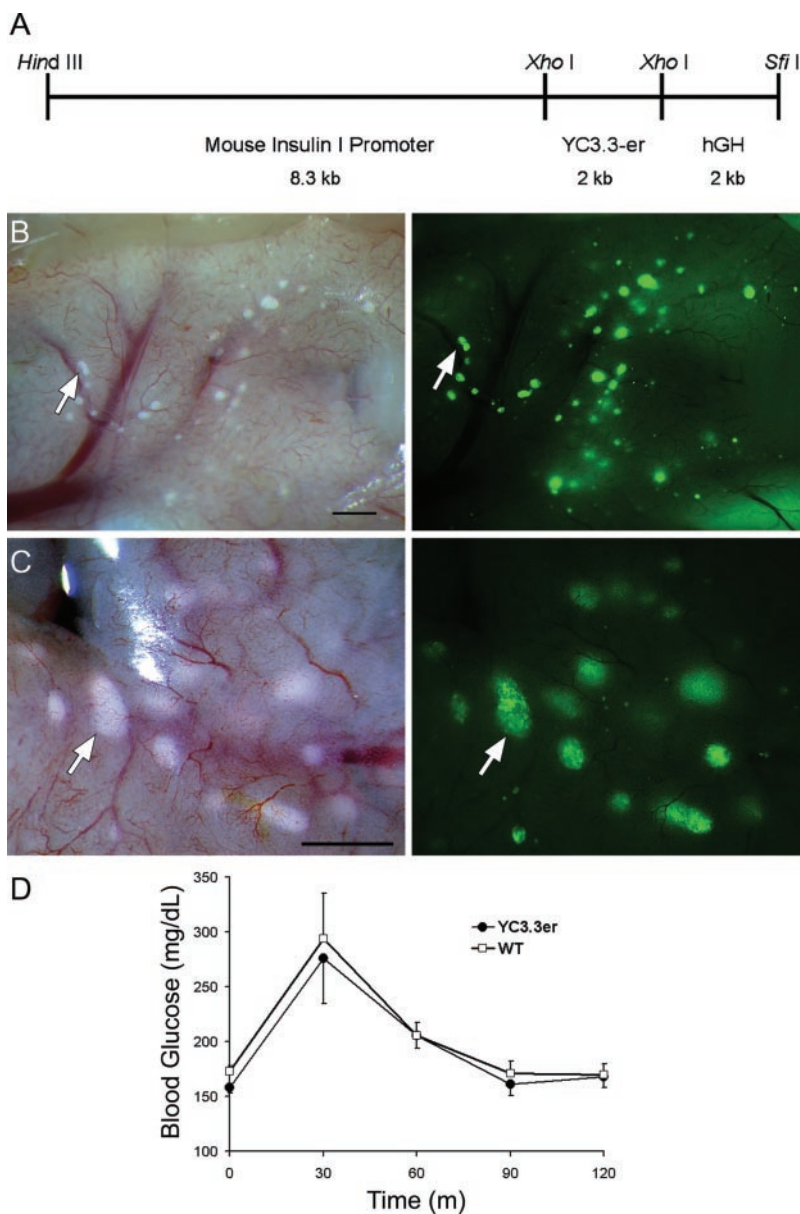


Fig. 1. Mouse insulin I gene promoter (MIP)-yellow cameleon3.3er (YC3.3-er) transgenic mice. *A*: diagram of the transgene construct of MIP-YC3.3er. hGH, human growth hormone. *B*: stereomicroscopic images of YC3.3-er expression in situ. An image of a portion of an intact pancreas of a 9-wk-old MIP-YC3.3-er transgenic mouse is shown. *Left*: the pancreas illuminated with white light. Note the appearance of numerous pale-appearing islets (arrow) near the surface of the pancreas. *Right*: the same field of view using fluorescence illumination and optical filters for visualizing yellow fluorescent protein. Scale bar indicates 1 mm. *C*: higher-magnification view of transgenic islet distribution in situ using white (*left*) and fluorescent (*right*) light. Individual islets of different sizes are easily visualized (arrow). Scale bar indicates 500 μ M. *D*: results of intraperitoneal glucose tolerance tests in 6-wk-old male MIP-YC3.3-er transgenic (YC3.3er) and CD-1 (wild type; WT) mice. No significant differences in blood glucose levels at each time point were observed ($P > 0.05$).

2G) colocalized with GRP94, a marker of ER (Fig. 2, *H-I*). This finding indicates that the transgenic biosensor is expressed within the lumen of the ER.

Fluorescence from individual cells within isolated live islets was easily detected (Fig. 3). The intensities of the fluorescent emission from the FRET donor and acceptor channels were very bright, ranging between 3- and 10-fold higher than the background autofluorescence observed in islets from control mice. YC3.3-er fluorescence was distributed throughout the cytoplasm of individual cells in a reticulated pattern (Fig. 3A) and analogous to the distribution of ER-targeted cameleon, YC4-er, in transiently transfected insulin-secreting cell lines (19). Intracellular expression of the biosensor was evident in the β -cells, characterized by membrane-bound lamellar and branching tubular structures contiguous with the ER and nuclear envelope (Fig. 3, *B-C*). The morphology of these structures in primary β -cells was strikingly similar to a nucleoplasmic

reticulum found in SKHep1 epithelial cells that is thought to regulate highly localized intranuclear Ca^{2+} signaling (4). Similar to what we observed in paraffin-embedded sections of transgenic mouse pancreas (Fig. 2), not all cells within the isolated islets expressed YC3.3-er. Nonfluorescent cells appeared as dark voids or cavities within the islets (Fig. 3, *B-D*) and likely represent α -cells, δ -cells, and PP cells of the endocrine pancreas. This conclusion is consistent with immunohistochemical studies showing an absence of transgenic GFP expression in other endocrine cell types within islets from MIP-GFP mice (7).

Our confocal imaging studies demonstrated intercellular and intracellular heterogeneity of the FRET emission intensity ratio in unstimulated islets (Fig. 3D). In some cells, the perinuclear ER appeared to exhibit a higher FRET ratio than the ER in the cytoplasm (Fig. 3D, *arrow*). These observations raise the possibility that the FRET ratio heterogeneity might reflect regional variations in ER Ca^{2+} levels and

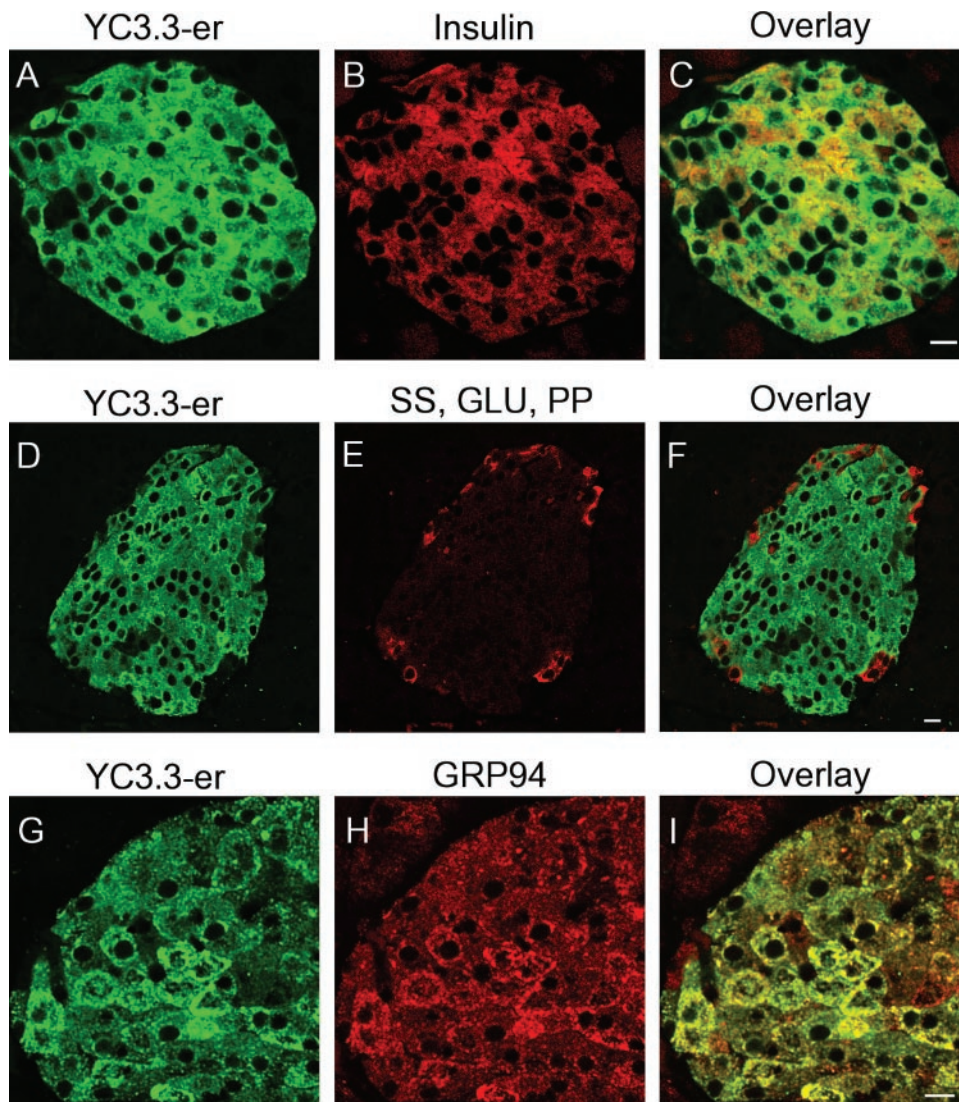


Fig. 2. Localization of YC3.3-er in transgenic mouse pancreas. Confocal images of immunostained islets and acinar tissue in paraffin-embedded pancreas sections. A–C: pattern of anti-green fluorescent protein (GFP) (A; YC3.3-er, green) and anti-insulin (B; Insulin, red) immunostaining in MIP-YC3.3-er mouse pancreatic tissue. The merged image (C; Overlay) shows extensive colocalization (yellow) of YC3.3-er and insulin in the islet. The red fluorescence in the surrounding acinar tissue is due to a low-level nonspecific background fluorescence resulting from staining paraffin-embedded sections with a Texas red-conjugated secondary antibody. D–F: section of pancreas stained with anti-GFP (D; YC3.3-er, green) and a combination of anti-somatostatin (SS), anti-glucagon (GLU), and anti-pancreatic polypeptide (PP) antibodies (E; red). In the merged image (F; Overlay), note the absence of overlapping immunostaining with anti-GFP (green) and the presence of non- β -cells (red) on the periphery of the islet. G–I: section of MIP-YC3.3-er mouse pancreas stained with anti-GFP (G; YC3.3-er, green) and anti-glucose-regulated protein 94 (H; GRP94, red) antibodies. The merged image reveals complete colocalization (yellow) of YC3.3-er and the endoplasmic reticulum (ER) marker in the islet (I; Overlay). Note the presence of an acinar cell adjacent to the islet immunostained with anti-GRP94 (H and I). A–I: scale bar indicates 10 μM .

suggest that β -cell ER Ca^{2+} is regulated by different mechanisms in distinct subcellular regions. More work will need to be done to explore these hypotheses.

We next determined whether the transgenic biosensor was functional. Cameleon indicators rely on Ca^{2+} -dependent FRET between chromophores of two GFP mutants as the basis for optical measurements of Ca^{2+} gradients (1, 6, 13, 17). The GFP mutants in YC3.3-er are ECFP and citrine, a mutant of enhanced yellow fluorescent protein (6). As Ca^{2+} concentration ($[\text{Ca}^{2+}]$) rises, FRET between ECFP and citrine increases, causing fluorescence emission from ECFP to decrease and citrine to increase. In contrast, a fall in $[\text{Ca}^{2+}]$ reduces FRET, and consequently ECFP emission intensity increases and citrine decreases. The ratio of citrine (FRET acceptor) and ECFP (FRET donor) fluorescence emission is indicative of $[\text{Ca}^{2+}]$. We measured FRET between ECFP and citrine in individual β -cells within intact transgenic islets visualized (at 10-s intervals) with a real-time spinning disk confocal microscope. Approximately 50–60 s after application of thapsigargin, an inhibitor of sarco(endo)plasmic reticulum Ca^{2+} -ATPases that causes irreversible depletion of Ca^{2+} sequestered within the ER

(18), biosensor FRET (Fig. 4A) and the ratio of FRET acceptor-to-donor emission decreased (Fig. 4B). This effect was observed in every cell ($n = 20$) we examined within transgenic islets expressing YC3.3-er (Fig. 4C) and indicated that MIP-YC3.3-er was providing a readout of changes in ER $[\text{Ca}^{2+}]$ ($[\text{Ca}^{2+}]_{\text{er}}$). This conclusion was further substantiated by exposing islets to carbachol, a muscarinic agonist that discharges ER Ca^{2+} stores by phospholipase C-mediated production of inositol 1,4,5-trisphosphate (IP_3) and activation of IP_3 receptor Ca^{2+} channels located in the ER membrane. Administration of carbachol transiently lowered $[\text{Ca}^{2+}]_{\text{er}}$, but not to the same extent as thapsigargin (Fig. 4D). The nadir of the carbachol-induced decrease in $[\text{Ca}^{2+}]_{\text{er}}$ occurred within 1 min and then ER Ca^{2+} increased and, after 5–6 min, returned to baseline levels. This is consistent with ER store refilling and likely reflects activation of thapsigargin-sensitive sarco(endo)plasmic reticulum Ca^{2+} -ATPases. However, we were surprised to observe that after depletion of ER Ca^{2+} stores by prolonged exposure of islets to thapsigargin (5 μM for 8 min) in solutions containing 2 mM glucose, administration of 20 mM glucose increased the average FRET ratio by 79% ($n =$

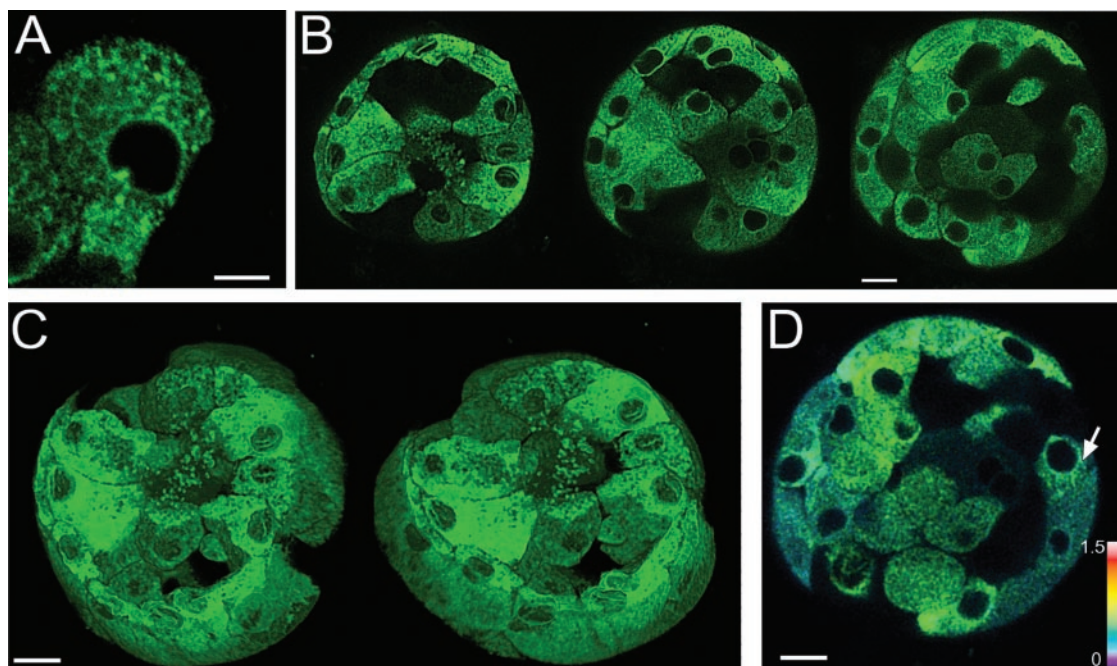


Fig. 3. Transgenic expression of YC3.3-er in islets of Langerhans. *A*: high-magnification confocal image of YC3.3-er fluorescence in a single β -cell inside an intact islet. Note the spiral structure connecting the reticulations in the cytosol and the nuclear envelope. White scale bar indicates 5 μM . *B*: confocal optical sections through a living isolated islet showing reticulated localization of YC3.3-er fluorescence inside β -cells. Localization includes the nuclear envelope and prominent invaginations into the nuclear region that may represent nucleoplasmic reticulum recently described in SKHep1 cells (4). Optical sections were collected at depths of 0.97, 7.23, and 13.25 μm (left to right, respectively) from the base of the islet. The mosaic appearance of the fluorescence likely indicates the location of α -cells, δ -cells, or pancreatic polypeptide-secreting cells that do not express the transgene under the control of the β -cell-specific MIP promoter. White scale bar indicates 50 μM . *C*: spatial localization of β -cells within an islet of Langerhans. Three-dimensional reconstruction of YC3.3-er distribution within 62 optical sections collected from islet shown in *B*. The 2 reconstructions differ by ~ 25 degrees, rotated in the z -plane. White scale bar indicates 50 μM . *D*: intensity-modulated display of fluorescence resonance energy transfer (FRET) acceptor (citrine) and donor (EYFP) images reveals intercellular variations of β -cell ER Ca^{2+} levels as well as intracellular gradients (arrow). White scale bar indicates 50 μM .

6 cells). This unexpected finding suggests that primary mouse β -cells possess a glucose-stimulated, thapsigargin-insensitive mechanism capable of refilling ER Ca^{2+} stores. The underlying mechanism remains to be determined.

DISCUSSION

Elucidating precisely how Ca^{2+} and other signaling molecules are organized and integrated dynamically to influence mammalian cell function in tissues and organ systems will be accomplished by measuring signal transduction events in situ. Problems with loading cells in thick biological tissues, and the lack of cell and subcellular compartment specificity of synthetic polycarboxylate Ca^{2+} dyes such as fura-2, preclude their use for ex vivo or in vivo imaging of Ca^{2+} signaling within intact multicellular mammalian organ systems. Although transgenically expressed fluorescent Ca^{2+} biosensors are potential candidates for quantitative real-time visualization of signaling in mammalian tissues, transgenic expression of GFP- and calmodulin-based cameleon and camgarrò indicators has been restricted to nonmammalian organisms (5, 9–11, 16, 20, 21).

The reasons for the difficulty in development of mammalian transgenic biosensor models are unclear. It has been proposed that a high level of expression is necessary for the detection of cameleon fluorescence and that biosensor over-

expression interferes with endogenous calmodulin-dependent signal transduction (17). On the other hand, interactions between yellow cameleon biosensors and endogenous calmodulin or calmodulin-binding proteins are unlikely; the major effect of overexpression is to increase Ca^{2+} buffering (12). An intracellular concentration of 20 μM is sufficient to detect cameleon fluorescence, and in vitro studies suggest that as much as 1 mM cameleon does not perturb calmodulin-dependent signaling (12). An alternate explanation for the failure of transgenic expression of protein-based Ca^{2+} biosensors in mammals might be the strategy employed to create the transgenic model. Our initial efforts to generate transgenic Ca^{2+} biosensor mice using a pancellular approach, driving transgene expression by β -actin or cytomegalovirus promoters, failed. Attempts to produce transgenic YC2.1 mice, a cameleon that measures cytoplasmic Ca^{2+} , resulted in embryonic lethality or insufficient levels of expression for detection (M. W. Roe and M. Rincon, unpublished observations). Tissue-specific targeting of YC3.3er resulted in the generation of transgenic mice with brightly fluorescent cells that were easily visualized (Fig. 1, *B* and *C*). Our studies indicate that mice tolerate expression of a GFP/calmodulin-based Ca^{2+} biosensor throughout maturation from neonate to adult without impairing the physiology of the transgenically targeted cells. The absence of a

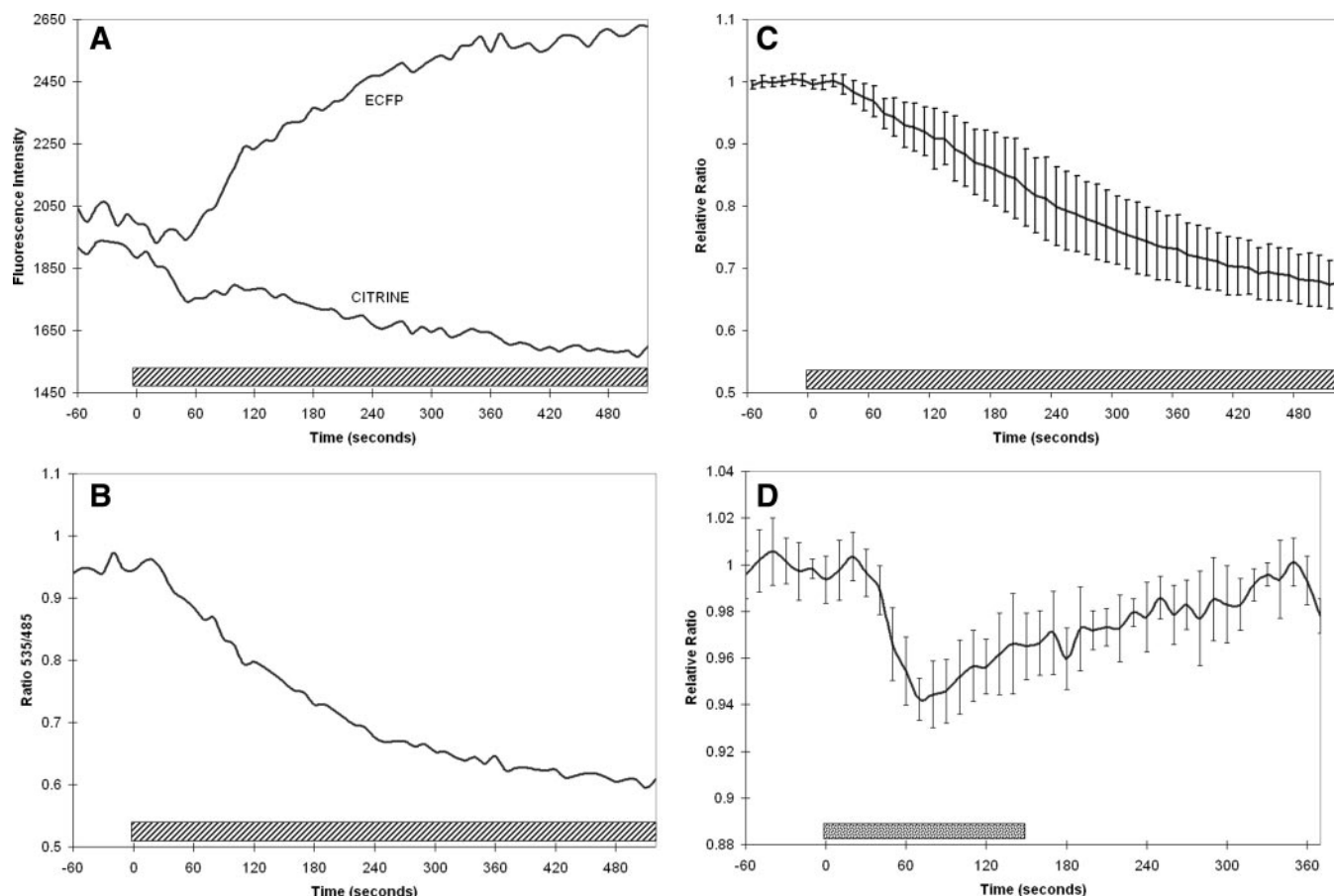


Fig. 4. Real-time confocal imaging of Ca^{2+} biosensor function in intact islets isolated from MIP-YC3.3-er transgenic mice. **A:** YC3.3-er FRET donor (ECFP) and acceptor (citrine) fluorescence after application of thapsigargin (hatched bar, $5 \mu\text{M}$). Traces illustrate time-dependent changes in the average fluorescence intensities of YC3.3-er detected at 485 nm (ECFP) and 535 nm (citrine) from a single β -cell in an intact islet of Langerhans imaged using confocal microscopy. Note that the fluorescence signals move in opposite directions: ECFP fluorescence increases and citrine emission decreases after drug treatment, reflecting a decrease in FRET between the 2 fluorescent components of the Ca^{2+} biosensor. **B:** ratio of the FRET acceptor and donor fluorescence emission (Ratio 535/485) measured in the cell from **A**. The decrease in the ratio indicates a decrease in ER Ca^{2+} concentration and is consistent with depletion of the ER Ca^{2+} stores after sarco(endo)plasmic reticulum Ca^{2+} -ATPase inhibition by thapsigargin (hatched bar, $5 \mu\text{M}$). **C:** average response of multiple β -cells in a single intact islet of Langerhans after application of thapsigargin (hatched bar, $5 \mu\text{M}$). Data are expressed as Ratio 535/485 normalized to average baseline ratio values measured 1 min before thapsigargin exposure (Relative Ratio). The mean ± 1 SD response of β -cells is shown ($n = 20$). **D:** effect of carbachol (stippled bar, $500 \mu\text{M}$) on ER Ca^{2+} in multiple β -cells (mean ± 1 SD, $n = 22$) in an islet. Note that refilling of the ER Ca^{2+} stores began in the presence of carbachol and continued after the stimulus was removed.

detectable effect of the MIP-YC3.3-er transgene on whole animal carbohydrate regulation is similar to transgenic mice expressing GFP in β -cells (7). The primary physiological function of β -cells is blood glucose sensing and insulin secretion, and it is well known that these processes are critically dependent on precise regulation of intracellular Ca^{2+} signaling (8). The findings suggest that MIP-YC3.3-er expression levels in the transgenic mice do not affect endogenous calmodulin-dependent physiological processes *in vivo*. This hypothesis is in close agreement with *in vitro* evidence from previous studies of the cameleons (12).

In the present study, we have established that a genetically encoded functional fluorescent Ca^{2+} biosensor can be expressed transgenically in intact mammalian tissues and engineered to label specific cells within a multicellular organ system. Our results suggest that cell-specific targeting of GFP-based biosensors is a feasible approach to generate transgenic

expression in mammals. It is conceivable that this approach could be adapted to exploit new biosynthetic fluorescent sensor designs as they become available and advance real-time optical analysis of signal transduction and cellular biochemistry in complex organ systems of living animals.

ACKNOWLEDGMENTS

We thank Dr. Roger Y. Tsien for generously providing YC3.3-er plasmid and Dr. Graeme I. Bell and Dr. Louis H. Philipson for numerous helpful discussions and support during the course of this project. Restituto Dizon provided excellent technical assistance in maintaining our transgenic cameleon mouse colonies.

GRANTS

This work was supported by the American Diabetes Association and National Institute of Diabetes and Digestive and Kidney Diseases Grants DK-64162 and DK-63493.

REFERENCES

1. Baird GS, Zacharias DA, and Tsien RY. Circular permutation and receptor insertion within green fluorescent proteins. *Proc Natl Acad Sci USA* 96: 11241–11246, 1999.
2. Berridge MJ, Lipp P, and Bootman MD. The versatility and universality of calcium signaling. *Nat Rev Mol Cell Biol* 1: 11–21, 2000.
3. Carofoli E, Santella L, Branca D, and Brini M. Generation, control, and processing of cellular calcium signals. *Crit Rev Biochem Mol Biol* 36: 107–260, 2001.
4. Echevarria W, Leite MF, Guerra MT, Zipfel WR, and Nathanson MH. Regulation of calcium signals in the nucleus by a nucleoplasmic reticulum. *Nat Cell Biol* 5: 440–446, 2003.
5. Fiala A, Spall T, Diegelmann S, Eisermann B, Sachse S, Devaud JM, Buchner E, and Galizia CG. Genetically expressed cameleon in *Drosophila melanogaster* is used to visualize olfactory information in projected neurons. *Curr Biol* 12: 1877–1884, 2002.
6. Griesbeck O, Baird GS, Campbell RE, Zacharias DA, and Tsien RY. Reducing the environmental sensitivity of yellow fluorescent protein: mechanisms and applications. *J Biol Chem* 276: 29188–29194, 2001.
7. Hara M, Wang X, Kawamura T, Bindokas VP, Dizon RF, Alcoser SY, Magnuson MA, and Bell GI. Transgenic mice with green fluorescent protein-labeled pancreatic β -cells. *Am J Physiol Endocrinol Metab* 284: E177–E183, 2003.
8. Henquin JC, Ishiyama N, Nenquin M, Ravier MA, and Jonas JC. Signals and pools underlying biphasic insulin secretion. *Diabetes* 51, Suppl 1: S60–S67, 2002.
9. Higashijima S, Masino MA, Mandel G, and Fetcho JR. Imaging neuronal activity during Zebrafish behavior with a genetically encoded calcium indicator. *J Neurophysiol* 90: 3986–3997, 2003.
10. Kerr R, Lev-Ram V, Baird G, Vincent P, Tsien RY, and Schafer WR. Optical imaging of calcium transients in neurons and pharyngeal muscle of *C. elegans*. *Neuron* 26: 583–594, 2000.
11. Lei L, Yermolaieva O, Johnson WA, Abboud FM, and Welsh MJ. Identification and function of thermosensory neurons in *Drosophila* larvae. *Nat Neurosci* 6: 267–273, 2003.
12. Miyawaki A, Griesbeck O, Heim R, and Tsien RY. Dynamic and quantitative Ca^{2+} measurements using improved cameleons. *Proc Natl Acad Sci USA* 96: 2135–2140, 1999.
13. Miyawaki A, Llopis J, Heim R, McCaffery JM, Adams JA, Ikura M, and Tsien RY. Fluorescent indicators for Ca^{2+} based on green fluorescent proteins and calmodulin. *Nature* 388: 882–887, 1997.
14. Palmiter RD, Sandgren EP, Avarbock MR, Allen DD, and Brinster RL. Heterologous introns can enhance expression of transgenes in mice. *Proc Natl Acad Sci USA* 88: 478–482, 1991.
15. Postic C, Shiota M, Niswender KD, Jetton TL, Chen Y, Moates JM, Shelton KD, Lindner J, Cherrington AD, and Magnuson MA. Dual roles for glucokinase in glucose homeostasis as determined by liver and pancreatic β cell-specific gene knock-outs using Cre recombinase. *J Biol Chem* 274: 305–315, 1999.
16. Reiff DF, Thiel PR, and Schuster CM. Differential regulation of active zone density during long-term strengthening of *Drosophila* neuromuscular junctions. *J Neurosci* 22: 9399–9409, 2002.
17. Rudolf R, Mongillo M, Rizzuto R, and Pozzan T. Looking forward to seeing calcium. *Nat Rev Mol Cell Biol* 4: 579–586, 2003.
18. Thomas D and Hanley MR. Pharmacological tools for perturbing intracellular calcium storage. *Methods Cell Biol* 40: 65–89, 1994.
19. Varadi A and Rutter GA. Dynamic imaging of endoplasmic reticulum Ca^{2+} concentration in insulin-secreting MIN6 cells using recombinant targeted cameleons: roles of sarco(endo)plasmic reticulum Ca^{2+} -ATPase (SERCA)-2 and ryanodine receptors. *Diabetes* 51, Suppl 1: S190–S201, 2002.
20. Wang JW, Wong AM, Flores J, Vossball LB, and Axel R. Two-photon calcium imaging reveals an odor-evoked map of activity in the fly brain. *Cell* 112: 271–282, 2003.
21. Yu D, Baird GS, Tsien RY, and Davis RL. Detection of calcium transients in *Drosophila* mushroom body neurons with camgaroos reporters. *J Neurosci* 23: 64–72, 2003.